

Communication

Pyrrolylquinoline-BF₂ and BPh₂ BODIPY-Type Analogues: Synthesis, Structural Analysis and Photophysical Properties

Abdulrahman A. Alsimaree^{1,2,*}, Omar M. Alatawi^{2,3}, Paul G. Waddell², David P. Day⁴, Nawaf I. Alsenani⁵ and Julian G. Knight² 

¹ Department of Basic Science (Chemistry) College of Science and Humanities, Shaqra University, Afif, P.O. Box 33, Shaqra 11961, Saudi Arabia

² School of Natural and Environmental Sciences, Bedson Building, Newcastle University, Newcastle upon Tyne NE1 7RU, UK; Omalatawi@gmail.com (O.M.A.); Paul.Waddell@newcastle.ac.uk (P.G.W.); julian.knight@newcastle.ac.uk (J.G.K.)

³ Department of Chemistry, Faculty of Science, University of Tabuk, Tabuk 47512, Saudi Arabia

⁴ São Carlos Institute of Chemistry, University of São Paulo, São Carlos 13560-970, SP, Brazil; davidpday@usp.br

⁵ Department of Chemistry, Faculty of Science, University of AlBaha, Alagig 65779-7738, Saudi Arabia; N.alsenani@bu.edu.sa

* Correspondence: alsimaree@su.edu.sa

Abstract: Two new pyrrolylquinoline-substituted heteroaromatic-containing compounds bearing a central boron bridge have been prepared by a short, high-yielding sequence consisting of Suzuki-coupling of 8-bromoquinoline and *N*-Boc 2-pyrroleboronic acid, thermolytic *tert*-butyloxycarbonyl deprotection, and subsequent boron chelation (either using boron trifluoride or triphenylborane). Both derivatives display longer wavelength absorption maxima ($\lambda_{\text{max}}^{\text{abs}}$) than a previously reported indolopyridine-BPh₂ analogue, in agreement with the smaller HOMO-LUMO energy gap predicted by DFT quantum chemical calculations. Both of the pyrrolylquinoline-boron chelates display weak emission (quantum yields 0.3–0.9%) and the BPh₂ complex displays a very broad, long-wavelength emission ($\lambda_{\text{max}}^{\text{em}} = 715 \text{ nm}$, MeCN), which may be due to dimer emission and results in a large pseudo-Stokes' shift (7753 cm^{-1}) for this compound.

Keywords: fluorescent molecules; structural analysis; boron bridged complex; DFT analysis; X-ray crystal analysis



Citation: Alsimaree, A.A.; Alatawi, O.M.; Waddell, P.G.; Day, D.P.; Alsenani, N.I.; Knight, J.G. Pyrrolylquinoline-BF₂ and BPh₂ BODIPY-Type Analogues: Synthesis, Structural Analysis and Photophysical Properties. *Crystals* **2021**, *11*, 1103. <https://doi.org/10.3390/cryst11091103>

Academic Editors: Assem Barakat and Alexander S. Novikov

Received: 26 August 2021

Accepted: 1 September 2021

Published: 10 September 2021

Publisher's Note: MDPI stays neutral with regard to jurisdictional claims in published maps and institutional affiliations.



Copyright: © 2021 by the authors. Licensee MDPI, Basel, Switzerland. This article is an open access article distributed under the terms and conditions of the Creative Commons Attribution (CC BY) license (<https://creativecommons.org/licenses/by/4.0/>).

1. Introduction

Since the initial report by Treibs and Kreuzer, who detailed the first examples of BODIPY derivatives [1], the field of chemistry associated with developing new fluorescent materials involving π -conjugated systems has drawn considerable attention across scientific boundaries [2–6]. The need for developing new fluorescent molecules is supported by the growing number of applications that they can be found in, for example, as metal or ion sensors [7–10], dyes used in laser spectroscopy [11–15], photo-labels in biological studies [16–20], incorporated into polymers [21,22], molecular rotors [23,24], amongst others. Over the past two decades, notable modifications to the core BODIPY structure have involved modification of the bridging boron atom (and replacement with other atoms) [25–27], addition of substituents around the pyrrole rings [28–30], substitution of the pyrrole rings for other hetero(carbo)aromatics to highlight just a few (Figure 1a) [31–33]. In some cases, a complete overhaul of the dye structure, yet keeping a tetrahedral boron(III) centre, has resulted in a number of novel dyes exhibiting unusual spectroscopic responses [34]. The fusion of quinoline derived units with either indoles [35], pyridines [36] and imidazoles [37], and subsequently formed as boron(III) complexes, has been reported in the literature (and their fluorescent properties studied). These findings built on the seminal work dating back to the late sixties, in which Hohaus reported the first quinoline-boron(III) complexes that

exerted photophysical properties [38]. Furthermore, important alternative heteroaromatics such as thiazole [39] or benzimidazole [37] have also been studied, along with the inclusion of quinoline carboxaldehydes to access numerous quinoline-containing BODIPY analogues (Figure 1b) [40].

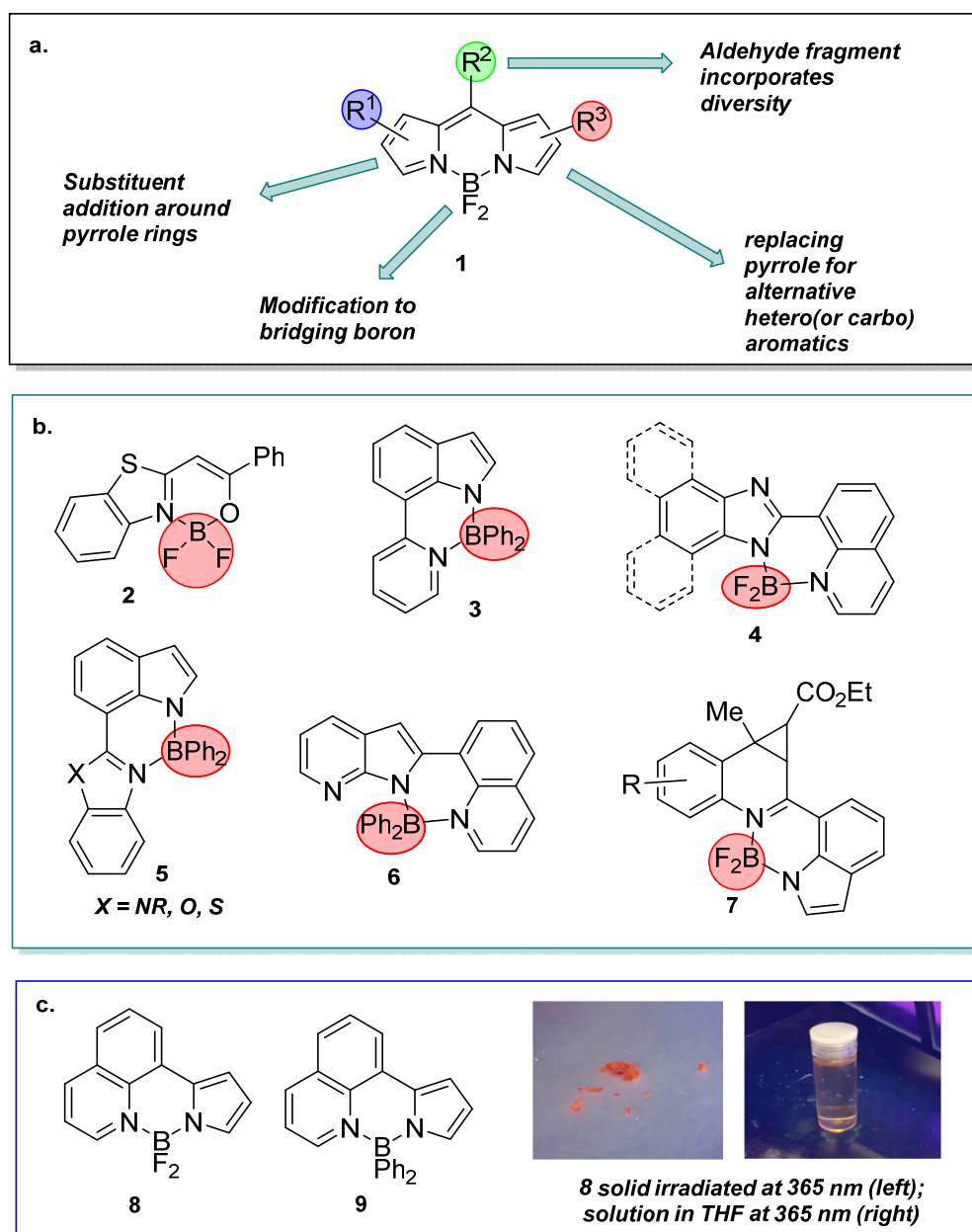


Figure 1. (a) Selected sites of modification to a classical BODIPY core **1**; (b) selected examples of BODIPY analogues bearing heteroaromatic moieties **2–7**; (c) structures of BF_2 and BPh_2 pyrrolylquinoline derivatives **8** and **9** included in this study, with images showing appearance under 365 nm light irradiation.

Despite these studies, to the best of our knowledge, the boron(III) chelated pyrrolylquinoline type fluorescent dyes shown in Figure 1c have not been reported. These are analogues of the simple pyridine-indole chelate **3** [41] in which the benzo-ring fusion has been transposed between the heteroaromatic cores. In this report, we detail the synthesis of such compounds using Suzuki coupling (bromo-quinoline-pyrrole boronic acid cross-coupling) as the initial step to build the core structure, followed by *N*-*tert*-butyloxycarbonyl removal

and subsequent boron complexation reactions to access the desired fluorophores. Along with full characterization of each compound (multi-nuclear NMR, X-ray, DFT, absorption and fluorescence analysis), we herein detail our findings.

2. Materials and Methods

General Methods: ^1H and ^{13}C NMR spectra were recorded directly with a Jeol Lambda 500 MHz, Jeol ECS-400 MHz or Bruker Avance 300 MHz. HRMS data were provided by the EPSRC National Mass Spectrometry Service (University of Swansea, UK). X-ray diffraction data were obtained on an Oxford Diffraction Gemini (Xcalibur, Atlas, Gemini ultra-diffractometer) and, using synchrotron radiation, on a Crystal Logics diffractometer fitted with a Rigaku Saturn detector (Xcalibur, Atlas, Gemini ultra-diffractometer equipped with a fine-focus sealed X-ray tube ($\lambda_{\text{CuK}\alpha} = 1.54184 \text{ \AA}$) and an Oxford Cryosystems CryostreamPlus open-flow N_2 cooling device. Rigaku Oxford Diffraction, 2015). IR spectra were obtained as neat samples using a Perkin Elmer L1600300, Spectrum Two LiTa FTIR spectrometer (Llantrisant, UK) scanning from $4000\text{--}600 \text{ cm}^{-1}$. THF and Et_2O were distilled from sodium/benzophenone and used directly. DCM was distilled from calcium hydride and used directly. Quantum chemical calculations were performed using the ORCA ab initio program [42]. Geometry optimizations and TD-DFT calculations were performed using the B3LYP functional, the def2-TZVPP basis set, RIJCOSX algorithm and the Conductor-like Polarizable Continuum Model (CPCM, acetonitrile).

2.1. 8-(1-tert-Butoxycarbonylpyrrol-2-yl)quinoline 12

N-Boc-2-pyrroleboronic acid (0.456 g, 2.16 mmol, 1.5 eq), 8-bromoquinoline (0.300 g, 1.44 mmol, 1 eq), K_3PO_4 (0.612 g, 2.88 mmol, 2 eq), and (2-dicyclohexylphosphino-2',4',6'-diisopropyl-1,1'-biphenyl)[2-(2'-amino-1,1'-biphenyl)]palladium(II) methanesulfonate (LPd(XPhos)OMs) (0.049 g, 0.057 mmol, 0.04 eq) were dissolved in dry THF (15 mL) and water (5 mL). The reaction mixture was heated under reflux for 6 h, then allowed to cool to room temperature. The mixture was diluted with CH_2Cl_2 (30 mL) and washed with water ($2 \times 10 \text{ mL}$). The organic solvent was dried over MgSO_4 and filtered. The organic solvent was removed under reduced pressure to yield an oil, which was purified by column chromatography (CH_2Cl_2) to give the title compound **12** as a dark oil (0.350 g, 1.19 mmol, 82%). ^1H NMR (300 MHz, CDCl_3): δ 8.73 (dd, $J = 4.2, 1.8 \text{ Hz}$, 1H), 7.96 (dd, $J = 8.3, 1.8 \text{ Hz}$, 1H), 7.62 (dd, $J = 8.2, 1.5 \text{ Hz}$, 1H), 7.57 (dd, $J = 7.1, 1.5 \text{ Hz}$, 1H), 7.40 (dd, $J = 3.1, 2.0 \text{ Hz}$, 1H), 7.37 (dd, $J = 8.2, 7.2 \text{ Hz}$, 1H), 7.18 (dd, $J = 8.2, 4.2 \text{ Hz}$, 1H), 6.26–6.11 (m, 2H), 0.80 (s, 9H). ^{13}C NMR (75 MHz, CDCl_3) δ 150.12, 149.60, 147.67, 136.00, 134.66, 132.16, 129.59, 128.06, 127.78, 126.14, 122.43, 121.02, 114.56, 110.60, 82.43, 27.20. IR (neat): $\nu_{\text{max}} / \text{cm}^{-1}$ 2980, 1733, 1593. HRMS-ES Calcd for $\text{C}_{18}\text{H}_{18}\text{N}_2\text{O}_2 + \text{H}^+$: 295.1440. Found: 295.1447.

2.2. 8-(Pyrrol-2-yl)quinoline 13

A round bottomed flask containing 8-(1-tert-butoxycarbonylpyrrol-2-yl)quinoline **12** (0.300 g, 1.02 mmol), was heated for 30 min at $200 \text{ }^\circ\text{C}$ under nitrogen resulting in the evolution of gas (presumed to be CO_2 , isobutene). The flask was then allowed to cool to room temperature. The crude product, a greenish solid, was directly used for the next reaction without purification (0.198 g, quant.). ^1H NMR (400 MHz, CDCl_3) δ 12.68 (br s, 1H), 8.93 (dd, $J = 4.3, 2.0 \text{ Hz}$, 1H), 8.18 (dd, $J = 8.2, 1.8 \text{ Hz}$, 1H), 8.16 (dd, $J = 8.2, 1.5 \text{ Hz}$, 1H), 7.63–7.53 (m, 2H), 7.42 (dd, $J = 6.2, 3.1 \text{ Hz}$, 1H), 7.09–7.05 (m, 1H), 6.96 (ddd, $J = 6.3, 4.2, 3.0 \text{ Hz}$, 1H), 6.38–6.42 (m, 1H). ^{13}C NMR (101 MHz, CDCl_3) δ 148.56, 144.61, 137.08, 131.63, 129.17, 129.09, 126.86, 125.04, 125.01, 120.77, 119.10, 108.97, 107.04.

2.3. 8,8-. Difluoro-8H-7I4,8I4-pyrrolo[1',2':3,4][1,3,2]diazaborinino[5,6,1-ij]quinolone 8

In a Schlenk tube, 8-(pyrrol-2-yl)quinoline (0.300 g, 1.54 mmol, 1 eq) was dissolved in CH_2Cl_2 (7 mL), diisopropylethylamine (1.16 g, 8.96 mmol, 5.8 eq) was added, followed by the addition of $\text{BF}_3 \cdot \text{Et}_2\text{O}$ (1.75 g, 12.4 mmol, 8 eq). The reaction mixture was stirred for 20 h. The solvent was then removed under reduced pressure to yield a solid, which was

purified by column chromatography (CH_2Cl_2) to give the title compound **8** as an orange solid (0.270 g, 1.11 g, 72%), mp = 163–165 °C. R_f = 0.6 (CH_2Cl_2). ^1H NMR (300 MHz, CDCl_3) δ 9.16 (d, J = 5.4, 1.6 Hz, 1H), 8.62 (dd, J = 8.3, 1.6 Hz, 1H), 8.17 (dd, J = 7.1, 1.8 Hz, 1H), 7.82–7.62 (m, 3H), 7.30 (dd, J = 2.6, 1.4 Hz, 1H), 6.91 (d, 1H), 6.45 (dd, J = 3.5, 2.5 Hz, 1H). ^{13}C NMR (75 MHz, CDCl_3) δ 145.10, 144.36, 129.70, 129.43, 127.67, 125.93, 125.41, 124.28, 123.60, 121.04, 111.75, 109.97, 108.05. ^{11}B NMR (96 MHz, CDCl_3) δ 1.85 (t, J = 29.3 Hz). ^{19}F NMR (282 MHz, CDCl_3) δ -140.05 (q, J = 29.3 Hz). IR (neat): $\nu_{\text{max}}/\text{cm}^{-1}$; 3062, 1588, 1510, 1378, 1299, 1259, 1209, 1138, 1107, 1065, 1039, 979, 879, 832, 738, 519. HRMS-ES Calcd for $\text{C}_{13}\text{H}_9\text{BF}_2\text{N}_2 + \text{H}^+$: 243.0905. Found: 243.0908.

2.4. 8,8-. Diphenyl-8H-7I4,8I4-pyrrolo[1',2':3,4][1,3,2]diazaborinino[5,6,1-ij]quinolone **9**

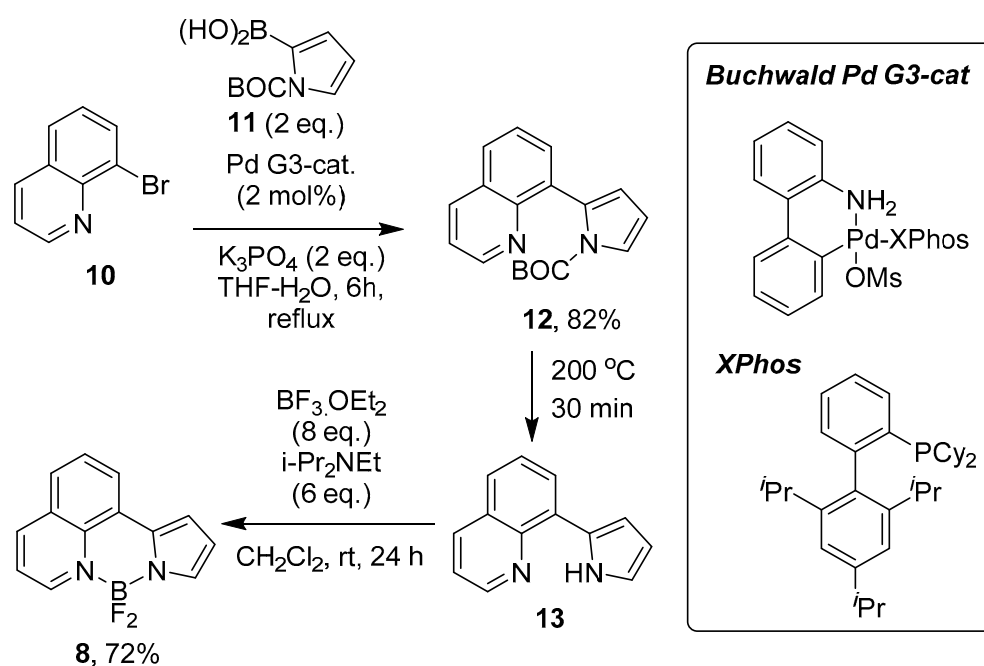
In a Schlenk tube, 8-(pyrrol-2-yl)quinoline (0.280 g, 1.44 mmol, 1.0 eq) **13** and triphenylborane (0.698 g, 2.88 mmol, 2.0 eq) were dissolved in toluene (10 mL). The reaction mixture was heated under reflux for 24 h and then allowed to cool to room temperature. The solvent was removed under reduced pressure to yield a solid, which was purified by column chromatography (CH_2Cl_2) to give the title compound **9** as a red solid (0.350 g, 0.97 mmol, 68%), mp 260–263 °C. R_f = 0.7 (CH_2Cl_2). ^1H NMR (300 MHz, CDCl_3) δ 8.76 (dd, J = 5.5, 1.6 Hz, 1H), 8.42 (dd, J = 8.3, 1.6 Hz, 1H), 8.12 (dd, J = 7.4, 1.5 Hz, 1H), 7.69–7.51 (m, 4H), 7.22–7.17 (m, 5H), 7.12–7.06 (m, 4H), 6.95 (dd, J = 3.5, 1.4 Hz, 1H), 6.68–6.66 (m, 1H), 6.37 (dd, J = 3.5, 2.4 Hz, 1H). ^{13}C NMR (75 MHz, CDCl_3) δ 147.01, 142.27, 136.58, 133.29, 129.95, 129.41, 128.93, 128.75, 128.31, 127.75, 127.47, 127.25, 127.17, 126.53, 124.06, 123.00, 120.32, 110.22, 107.60. ^{11}B NMR (96 MHz, CDCl_3) δ 4.05 (s). IR (neat): $\nu_{\text{max}}/\text{cm}^{-1}$; 3068, 3045, 1587, 1538, 1507, 1429, 1374, 1362, 1230, 1230, 1200, 1177, 1171, 1071, 872, 827, 725, 640, 619. HRMS-ES Calcd for $\text{C}_{25}\text{H}_{19}\text{BF}_2\text{N}_2 + \text{H}^+$: 359.1720. Found: 359.1726.

3. Results

3.1. Synthesis

The synthesis of both pyrrolylquinoline boron bridged analogues **8** and **9** requires access to intermediate **13** before boron complexation. We were pleased to find that Suzuki cross-coupling reaction between commercially available 8-bromoquinoline **10** and *N*-Boc pyrrole-2-boronic acid **11** employing Buchwald's Pd G3 pre-catalyst in combination with XPhos ligand (in 2:1 THF:H₂O) afforded cross-coupled product **12** in an excellent 82% yield (Scheme 1) [43]. A facile *tert*-butyloxycarbonyl deprotection could be realized by solvent-free heating at 200 °C under inert atmosphere to yield the carbamate **12**. Thermolytic cleavage of the *tert*-butyl group, followed by decarboxylation, affords the NH-pyrrole **13** in an essentially quantitative yield (along with isobutene and carbon dioxide as additional products). The desired BF₂-chelated pyrrolylquinoline derivative **8** was formed from the pyrrole **13** in 72% yield by reaction with boron trifluoride etherate (8 equivalents) in the presence of Hünig's base (6 equivalents).

To confirm the structure of BF₂-chelated pyrrolylquinoline compound **8**, we initially investigated multi-nuclear NMR analysis for this product (see Supplementary Materials for details of ^1H , ^{13}C , ^{19}F and ^{11}B NMR spectroscopy). Characteristically, ^{19}F NMR indicated a solitary signal at -140 ppm, with the expected quartet observed due to F-B coupling (Figure 2a). Likewise, the ^{11}B NMR spectrum showed a triplet at δ 1.85 ppm for the BF₂-group (Figure 2b). The boron chelate **8** was crystallized from a solvent system of chloroform and diethyl ether (1:3) and the molecular structure was confirmed by single crystal X-ray diffraction. The bond angle 107.72° (N9-B8-N7) for **8** is close to tetrahedral and similar to the corresponding angle 106.6° (N2-B4-N1) in a typical unsubstituted BODIPY **1** (see Figure 1a) [44]. This suggests that there is no induced strain on the aromatic system of **8** (Figure 2).



Scheme 1. Synthesis of BF_2 -chelated pyrrolylquinoline **8**.

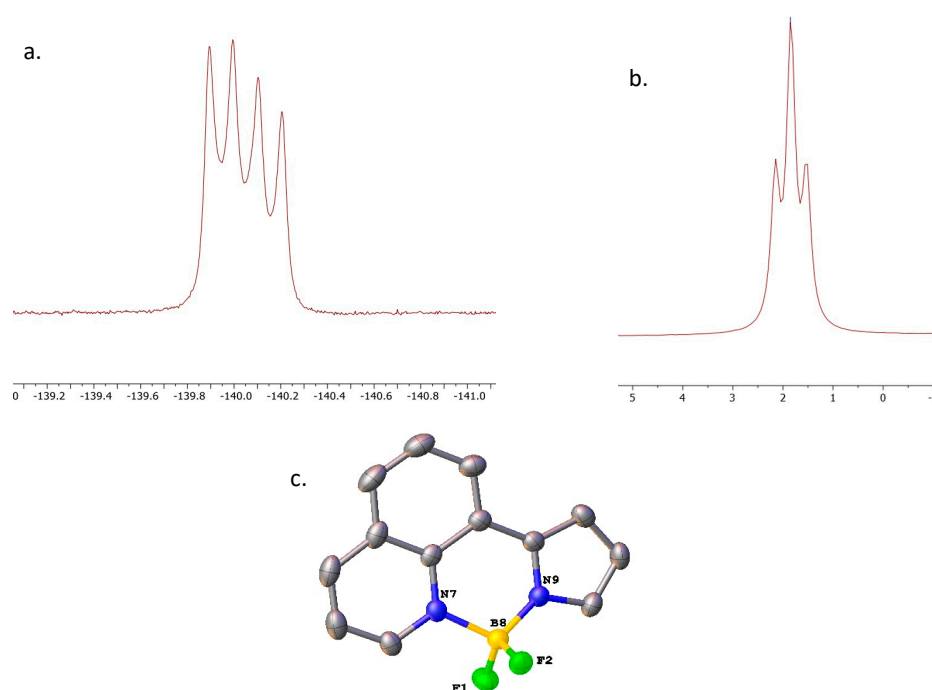
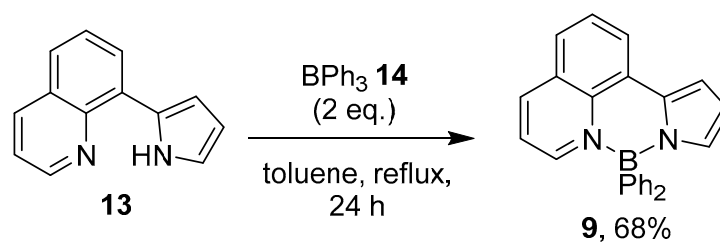


Figure 2. (a) ^{19}F NMR spectrum (282 MHz, CDCl_3) of the pyrrolylquinoline- BF_2 complex **8**. (b) ^{11}B NMR spectrum (96 MHz, CDCl_3) of the pyrrolylquinoline- BF_2 complex **8**. (c) X-ray single crystal analysis of pyrrolylquinoline- BF_2 complex **8** (hydrogen atoms have been omitted for clarity).

The corresponding pyrrolylquinoline BPh_2 complex **9** was accessed according to the procedure employed by Curiel and co-workers for the synthesis of the analogous indole **3** [41]. The pyrrolylquinoline intermediate **13** was treated with two equivalents of triphenylborane **14** in toluene under reflux. The BPh_2 chelate **9** was isolated in 68% yield (Scheme 2).



Scheme 2. BPh₂-chelation of pyrrolylquinoline intermediate **13**.

The successful formation of pyrrolylquinoline-BPh₂ **9** was confirmed by X-ray structure and by the ¹¹B NMR spectroscopy, showing the expected singlet peak at δ 4.05 ppm (Figure 3).

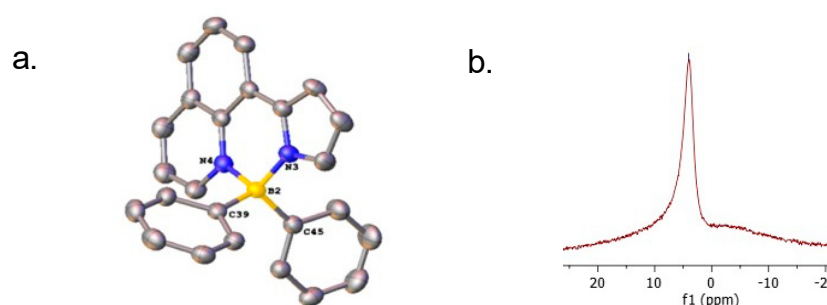


Figure 3. (a) X-ray crystal structure for BPh₂-adduct **9**. (Hydrogen atoms have been omitted for clarity). (b) ¹¹B NMR spectrum for **9** (96 MHz, CDCl₃).

3.2. Photophysical Properties and DFT Analysis

The UV-vis and emission spectra, measured in acetonitrile and tetrahydrofuran at room temperature, for the two quinoline-derived BODIPY-type analogues (BF₂) **8** and (BPh₂) **9** are shown in Figure 4 and the key parameters are summarized in Table 1 together with the previously reported [42] data for the ‘structurally transposed’ indolopyridine-BPh₂ analogue **3** for comparison. Fluorescein was used as the reference compound for the determination of luminescence quantum yield (fluorescein Φ_f = 0.925, λ_{ex} = 405 nm, in NaOH_(aq) (0.1 M)) [45].

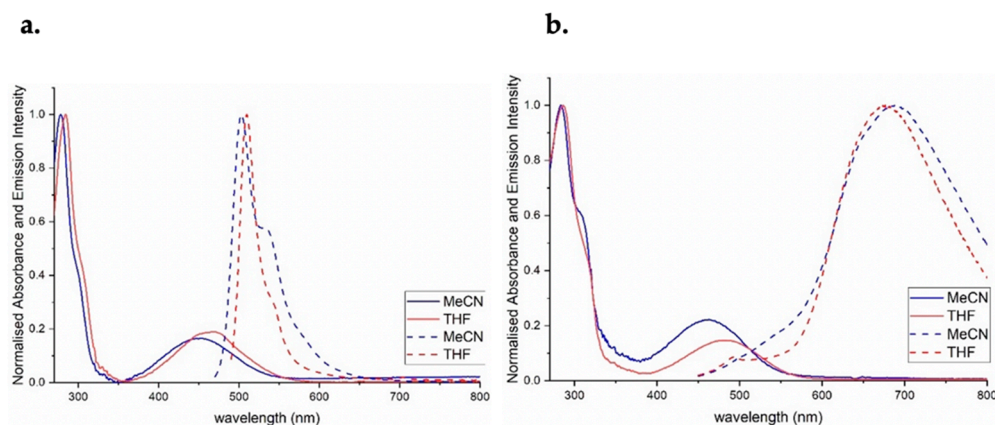


Figure 4. Normalized absorption (solid lines) and emission spectra (dashed lines) of (a) pyrrolylquinoline-BF₂ **8** and (b) -BPh₂ **9** in MeCN and THF.

Table 1. Photophysical data for the selected BODIPY analogues.

BODIPY Analogue	Solvent	λ_{abs} (max) /nm	$\epsilon/10^3 \text{ M}^{-1}$ cm^{-1}	λ_{em} (max) /nm	$\Delta\nu$ ^{SS} / cm^{-1} ^c	Φ_f (λ_{ex})
8	MeCN	278, 450	15, 2.8	503	2342	0.007 (405)
8	THF	284, 470	32, 5.5	510	1669	0.003 (405)
9	MeCN	283, 460	13, 3.2	715	7753	0.009 (405)
9	THF	286, 480	22, 4.0	693	6403	0.005 (405)
Indolopyridine BPh ₂ 3 ^a	MeCN	409	8.0	519	5182	0.12 ^b

^a Data taken from Reference [41]; ^b reported as determined in ethanol [41]; ^c Stokes' shift.

The UV-vis absorption spectrum of the BF₂ dye **8** in THF solution shows a strong absorption band at 284 nm and a weaker absorption at 470 nm (Figure 4). A weak fluorescence emission ($\varphi_f = 0.3\%$) is observed at 510 nm, and the appearance of the emission spectrum strongly resembles that of a typical BODIPY-F₂ dye [2–6]. An increase in solvent polarity (from THF to MeCN) results in a hypsochromic shift in both the absorption and (to a lesser extent) emission λ_{max} ; consequently, the Stokes' shift increases from 1669 to 2342 cm^{-1} (Table 1). The luminescence quantum yield also increases (to 0.7%) in the more polar solvent. The UV-vis absorption spectrum of BPh₂ pyrrolylquinoline chelate **9** is similar to that of the BF₂-chelate with absorption peaks at 286 and 480 nm in THF, which undergo hypsochromic shifts in MeCN (Figure 4). The emission spectrum of BPh₂ pyrrolylquinoline chelate **9** consists of a very broad, featureless peak at λ_{max} 693 nm in THF with a low quantum yield of emission (0.5%). In the more polar solvent MeCN, a bathochromic shift (λ_{max} 715 nm) and increase in quantum yield (0.9%) is observed. The excitation spectra for both chelates **8** and **9** closely match the absorption spectra, indicating that the emission arises from a single excited state in each case.

The emission behaviour of the BPh₂ chelate **9** is in stark contrast to that of the BF₂ chelate **8**, and it may correspond to emissions from a dimer in solution as a result of poor solubility of the BPh₂ chelate in THF and MeCN, favouring dimerization in solution. We were unable to observe more typical 'monomer-like' emission even on attempted serial dilutions. As a consequence of this unexpected low energy emission, the apparent Stokes shift (Table 1) is much larger than that for either the BF₂ chelate **8** or the reported indolopyridine analogue **3**. It is interesting to note that the reported emission spectrum of the indolopyridine **3** in acetonitrile does feature a broad peak, typical of a BPh₂-BODIPY [46], but this is centred at a much shorter wavelength (519 nm) than that observed for the isomeric quinoline chelate **9** [41].

Figure 5 shows the HOMO and LUMO orbitals and energies of these pyrrolylquinoline analogues **8** and **9** together with those for the indolopyridine isomer **3** for comparison, calculated using density functional theory (DFT) at the B3LYP/def2-TZVPP level, applying the conductor-like polarizable continuum model (CPCM, with solvent = MeCN) to account for solvent effects. As might be anticipated on the basis of the electronic nature of the ring systems, for both **8** and **9**, the HOMO is predominantly focused on the pyrrole and the carbocyclic ring of the quinoline, whereas the LUMO is predominantly focused on the quinoline rings. The HOMO-LUMO energy gaps for **8** and **9** are 2.97 eV in each case, which is substantially smaller than the HOMO-LUMO gap of 3.51 eV calculated for the indolopyridine **3** at the same level of theory and is in agreement with the significant red shift in the absorbance maximum of the pyrroloquinolines compared to the indole.

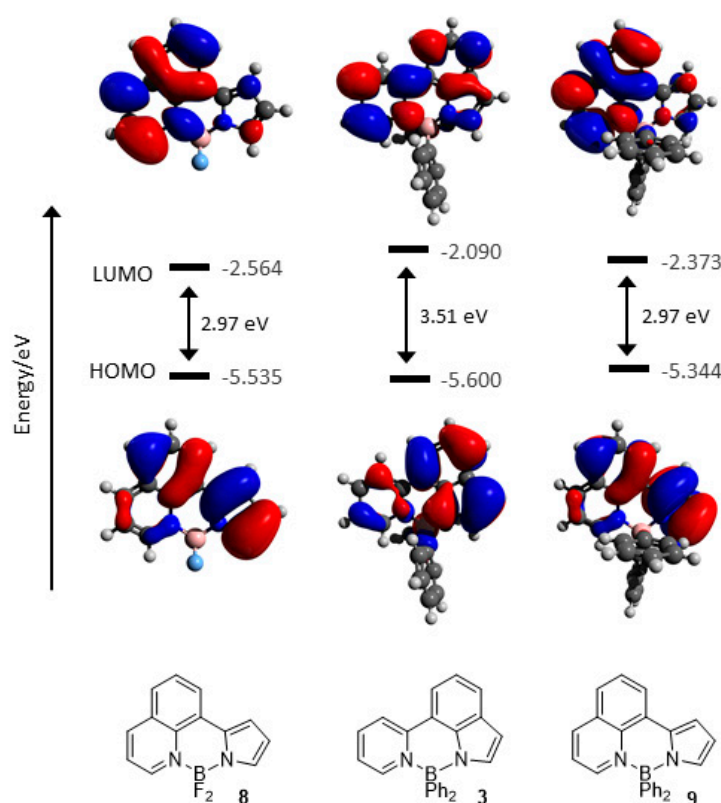


Figure 5. HOMO and LUMO molecular orbitals and energies (eV) for **8** and **9** together with those for the indolopyridine **3** for comparison. Calculated by DFT at the B3LYP/def2-TZVPP level using ORCA [42].

The principle absorption peak positions (those with $f_{\text{osc}} > 0.02$) were predicted by time-dependent DFT calculations (ESI). Peaks at 608 ($S_0 \rightarrow S_1$) and 278 nm ($S_0 \rightarrow S_5$) were predicted for the BF_2 -chelate **8**; at 594 ($S_0 \rightarrow S_1$) and 300 nm ($S_0 \rightarrow S_8$) for the BPh_2 -chelate **9**; and at 454 ($S_0 \rightarrow S_1$), 394 ($S_0 \rightarrow S_2$), 330 ($S_0 \rightarrow S_7$), and 272 nm ($S_0 \rightarrow S_{11}$) for the BPh_2 -chelate **3**, included for comparison. For the indolopyridine- BPh_2 chelate **3**, the calculated absorption spectrum is in reasonable agreement with the reported experimental results, as reported previously [41]. For the new pyrrolylquinoline-chelates **8** and **9**, $\lambda_{\text{max}}^{\text{abs}}$ is correctly predicted to occur at longer wavelengths than the indole **3**; however, the energy of this transition was significantly underestimated in both cases, leading to a longer wavelength prediction compared to the experimental result. Inspection of the molecular orbital contributions to all of these transitions confirms them to be $\pi \rightarrow \pi^*$ in nature.

4. Conclusions

Fluorescent boron-complexed dyes have become an area of intensive research due to their potential applications, which were discussed at the beginning of this article. Many approaches to the synthesis of boron(III)-complexed dyes have been reported in the literature, and we have adapted some of these in order to prepare a new core. The two new BODIPY-like pyrrolylquinoline boron-chelates **8** and **9** are prepared in good yields through a simple and short synthetic sequence, and their structures have been confirmed by means of single-crystal X-ray diffraction and multi-nuclear NMR spectroscopy. In comparison to the previously reported indolopyridine derivative **3**, which is isomeric to the pyrrole **9**, the quantum yields for both dyes were low. The emission spectrum of the difluoroboron compound **8** is typical for a heteroaromatic N,N,F,F -boron chelate but the BPh_2 -chelate **9** displayed only a very broad, highly red-shifted emission, which may be due to emissions from a dimer in solution and results in a large apparent Stokes' shift. We envisage future

boron(III) analogues to be developed further by adding different substituents to the pyrrole moiety that may enhance the photophysical properties of these complexes. This could be achieved by brominating certain positions on the pyrrole ring, and then incorporating new aromatic or heteroatom moieties via a Suzuki cross-coupling. The apparent emission from an aggregate, in the BPh₂ chelate **9**, may warrant further investigation.

Supplementary Materials: Supplementary materials are available online at <https://www.mdpi.com/article/10.3390/cryst11091103/s1>.

Author Contributions: Conceptualization, J.G.K.; methodology, A.A.A.; investigation, A.A.A., O.M.A.; writing—J.G.K., A.A.A., P.G.W., D.P.D.; writing—review and editing, J.G.K., D.P.D., A.A.A., N.I.A.; supervision, J.G.K. All authors have read and agreed to the published version of the manuscript.

Funding: This research received no external funding.

Acknowledgments: A.A.A. wishes to thank Newcastle University and Shaqra University for funding and support. O.M.A. thanks Newcastle University and Tabuk University for support.

Conflicts of Interest: The authors declare no conflict of interest.

References

1. Treibs, A.; Kreuzer, F.-H. Difluoroboryl-Komplexe von Di- und Tripyrrylmethenen. *Liebigs Ann. Chem.* **1968**, *718*, 208–223. [[CrossRef](#)]
2. Ziessel, R.; Ulrich, G.; Harriman, A. The chemistry of Bodipy: A new El Dorado for fluorescence tools. *New J. Chem.* **2007**, *31*, 496–501. [[CrossRef](#)]
3. Ulrich, G.; Ziessel, R.; Harriman, A. The Chemistry of Fluorescent Bodipy Dyes: Versatility Unsurpassed. *Angew. Chem. Int. Ed.* **2008**, *47*, 1184–1201. [[CrossRef](#)] [[PubMed](#)]
4. Lu, H.; Shen, Z. BODIPYs and their derivatives: The past, present and future. *Front. Chem.* **2020**, *8*, 290. [[CrossRef](#)]
5. Squeo, B.M.; Pasini, M. BODIPY platform: A tunable tool for green to NIR OLEDs. *Supramol. Chem.* **2020**, *32*, 56–70. [[CrossRef](#)]
6. Loudet, A.; Burgess, K. BODIPY dyes and their derivatives: Syntheses and spectroscopic properties. *Chem. Rev.* **2007**, *107*, 4891–4932. [[CrossRef](#)]
7. Niu, L.-Y.; Li, H.; Feng, L.; Guan, Y.-S.; Chen, Y.-Z.; Duan, C.-F.; Wu, L.-Z.; Guan, Y.-F.; Tung, C.-H.; Yang, Q.-Z. BODIPY-based fluorometric sensor array for the highly sensitive identification of heavy-metal ions. *Anal. Chim. Acta* **2013**, *775*, 93–99. [[CrossRef](#)] [[PubMed](#)]
8. Sun, W.; Chen, R.; Cheng, X.; Marin, L. Bodipy-based chemosensors for highly sensitive and selective detection of Hg²⁺ ions. *New J. Chem.* **2018**, *42*, 19224–19231. [[CrossRef](#)]
9. Baslak, C.; Kursunlu, A.N. A naked-eye fluorescent sensor for copper (II) ions based on a naphthalene conjugate Bodipy dye. *Photochem. Photobiol. Sci.* **2018**, *17*, 1091–1097. [[CrossRef](#)]
10. Özcan, E.; Çosut, B. Fluorescent Sensing of Cesium Ions by an Amide-Linked BODIPY Dye: Synthesis and Photophysical Properties. *ChemistrySelect* **2018**, *3*, 7940–7944. [[CrossRef](#)]
11. Bañuelos, J.; Martín, V.; Azael Gómez-Durán, C.F.; Arroyo Córdoba, I.J.; Peña-Cabrera, E.; García-Moreno, I.; Costela, Á.; Pérez-Ojeda, M.E.; Arbeloa, T.; Arbeloa, I.L. New 8-Amino-BODIPY derivatives: Surpassing laser dyes at blue-edge wavelengths. *Chem. Eur. J.* **2011**, *17*, 7261–7270. [[CrossRef](#)]
12. García, O.; Sastre, R.; del Agua, D.; Costela, A.; García-Moreno, I.; López Arbeloa, F.; Bañuelos Prieto, J.; López Arbeloa, I. Laser and physical properties of BODIPY chromophores in new fluorinated polymeric materials. *J. Phys. Chem. C* **2007**, *111*, 1508–1516. [[CrossRef](#)]
13. Kölmel, D.K.; Hörner, A.; Castañeda, J.A.; Ferencz, J.A.P.; Bihlmeier, A.; Nieger, M.; Bräse, S.; Padilha, L.A. Linear and nonlinear optical spectroscopy of fluoroalkylated BODIPY dyes. *J. Phys. Chem. C* **2016**, *120*, 4538–4545. [[CrossRef](#)]
14. Maity, A.; Sarkar, A.; Patra, S.K. Design and synthesis of perfluoroalkyl decorated BODIPY dye for random laser action in a microfluidic device. *New J. Chem.* **2020**, *44*, 14650–14661. [[CrossRef](#)]
15. Ortiz, M.J.; Garcia-Moreno, I.; Agarrabeitia, A.R.; Duran-Sampedro, G.; Costela, A.; Sastre, R.; López Arbeloa, F.; Bañuelos Prieto, J.; López Arbeloa, I. Red-edge-wavelength finely-tunable laser action from new BODIPY dyes. *Phys. Chem. Chem. Phys.* **2010**, *12*, 7804–7811. [[CrossRef](#)]
16. Kaur, P.; Singh, K. Recent advances in the application of BODIPY in bioimaging and chemosensing. *J. Mater. Chem.* **2019**, *7*, 11361–11405. [[CrossRef](#)]
17. Ni, Y.; Wu, J. Far-red and near infrared BODIPY dyes: Synthesis and applications for fluorescent pH probes and bio-imaging. *Org. Biomol. Chem.* **2014**, *12*, 3774–3791. [[CrossRef](#)] [[PubMed](#)]
18. Zlatić, K.; Antol, I.; Uzelac, L.; Mikecin Dražić, A.-M.; Kralj, M.; Bohne, C.; Basarić, N. Labeling of Proteins by BODIPY-Quinone Methides Utilizing Anti-Kasha Photochemistry. *ACS Appl. Mater. Interfaces* **2020**, *12*, 347–351. [[CrossRef](#)] [[PubMed](#)]

19. Donnelly, J.L.; Offenbartl-Stiegert, D.; Marín-Beloqui, J.M.; Rizzello, L.; Battaglia, G.; Clarke, T.M.; Howorka, S.; Wilden, J.D. Exploring the Relationship between BODIPY Structure and Spectroscopic Properties to Design Fluorophores for Bioimaging. *Chem. Eur. J.* **2020**, *26*, 863–872. [[CrossRef](#)] [[PubMed](#)]
20. Koleman, S.; Akkaya, E.U. Reaction-based BODIPY probes for selective bio-imaging. *Coordin. Chem. Rev.* **2018**, *354*, 121–134. [[CrossRef](#)]
21. Squeo, B.M.; Gregoriou, V.G.; Avgeropoulos, A.; Baysec, S.; Allard, S.; Scherf, U.; Chochos, C.L. BODIPY-based polymeric dyes as emerging horizon materials for biological sensing and organic electronic applications. *Prog. Polym. Sci.* **2017**, *71*, 26–52. [[CrossRef](#)]
22. Alemдарoglu, F.E.; Alexander, S.C.; Ji, D.; Prusty, D.K.; Börsch, M.; Herrmann, A. Poly (BODIPY) s: A new class of tunable polymeric dyes. *Macromolecules* **2009**, *42*, 6529–6536. [[CrossRef](#)]
23. Bahaidarah, E.; Harriman, A.; Stachelek, P.; Rihn, S.; Heyer, E.; Ziessele, R. Fluorescent molecular rotors based on the BODIPY motif: Effect of remote substituents. *Photochem. Photobiol. Sci.* **2014**, *13*, 1397–1401. [[CrossRef](#)]
24. Benniston, A.C.; Harriman, A.; Whittle, V.L.; Zelzer, M. Molecular rotors based on the boron dipyrromethene fluorophore. *Eur. J. Org. Chem.* **2010**, *2010*, 523–530. [[CrossRef](#)]
25. Boens, N.; Verbelen, B.; Ortiz, M.J.; Jiao, L.; Dehaen, W. Synthesis of BODIPY dyes through postfunctionalization of the boron dipyrromethene core. *Coordin. Chem. Rev.* **2019**, *399*, 213024. [[CrossRef](#)]
26. Boens, N.; Verbelen, B.; Dehaen, W. Postfunctionalization of the BODIPY core: Synthesis and spectroscopy. *Eur. J. Org. Chem.* **2015**, *2015*, 6577–6595. [[CrossRef](#)]
27. Lu, J.-S.; Ko, S.-B.; Walters, N.R.; Wang, S. Decorating BODIPY with three- and four-coordinate boron groups. *Org. Lett.* **2012**, *14*, 5660–5663. [[CrossRef](#)]
28. Kue, C.S.; Ng, S.Y.; Voon, S.H.; Kamkaew, A.; Chung, L.Y.; Kiewe, L.V.; Lee, H.B. Recent strategies to improve boron dipyrromethene (BODIPY) for photodynamic cancer therapy: An updated review. *Photochem. Photobiol. Sci.* **2018**, *17*, 1691–1708. [[CrossRef](#)] [[PubMed](#)]
29. Zhou, X.; Yu, C.; Feng, Z.; Yu, Y.; Wang, J.; Hao, E.; Wei, Y.; Mu, X.; Jiao, L. Highly regioselective α -chlorination of the BODIPY chromophore with copper (II) chloride. *Org. Lett.* **2015**, *17*, 4632–4635. [[CrossRef](#)] [[PubMed](#)]
30. Yu, C.; Miao, W.; Wang, J.; Hao, E.; Jiao, L. Effect of Short PEG on Near-Infrared BODIPY-Based Activatable Optical Probes. *ACS Omega* **2017**, *2*, 3551–3561. [[CrossRef](#)] [[PubMed](#)]
31. Wang, J.; Boens, N.; Jiao, L.; Hao, E. Aromatic [b]-fused BODIPY dyes as promising near-infrared dyes. *Org. Biomol. Chem.* **2020**, *18*, 4135–4156. [[CrossRef](#)]
32. Jiang, X.-D.; Gao, R.; Yue, Y.; Sun, G.-T.; Zhao, W. A NIR BODIPY dye bearing 3,4,4a-trihydroxanthene moieties. *Org. Biomol. Chem.* **2012**, *10*, 6861–6865. [[CrossRef](#)]
33. Shimizu, S.; Iino, T.; Araki, Y.; Kobayashi, N. Pyrrolopyrrole aza-BODIPY analogues: A facile synthesis and intense fluorescence. *Chem. Commun.* **2013**, *49*, 1621–1623. [[CrossRef](#)]
34. Frath, D.; Massue, J.; Ulrich, G.; Ziessele, R. Luminescent Materials: Locking π -Conjugated and Heterocyclic Ligands with Boron (III). *Angew. Chem. Int. Ed.* **2014**, *53*, 2290–2310. [[CrossRef](#)] [[PubMed](#)]
35. Luo, H.-X.; Niu, Y.; Jin, X.; Cao, X.-P.; Yao, X.; Ye, X.-S. Indolo-quinoline boron difluoride dyes: Synthesis and spectroscopic properties. *Org. Biomol. Chem.* **2016**, *14*, 4185–4188. [[CrossRef](#)] [[PubMed](#)]
36. Quan, L.; Chen, Y.; Lv, X.-J.; Fu, W.-F. Aggregation-Induced Photoluminescent Changes of Naphthyridine–BF₂ Complexes. *Chem. Eur. J.* **2012**, *18*, 14599–14604. [[CrossRef](#)] [[PubMed](#)]
37. Li, W.; Lin, W.; Wang, J.; Guan, X. Phenanthro[9,10-d]imidazole-quinoline Boron Difluoride Dyes with Solid-State Red Fluorescence. *Org. Lett.* **2013**, *15*, 1768–1771. [[CrossRef](#)]
38. Hohaus, E.; Umland, F. Borchelate und Bormetallchelate, I. Borchelate mit Chelatbildnern der Pyridin- und Chinolin-Reihe und ihren N-Oxiden. *Chem. Ber.* **1969**, *102*, 4025–4031. [[CrossRef](#)]
39. Kubota, Y.; Tanaka, S.; Funabiki, K.; Matsui, M. Synthesis and fluorescence properties of thiazole–boron complexes bearing a β -ketoiminate ligand. *Org. Lett.* **2012**, *14*, 4682–4685. [[CrossRef](#)] [[PubMed](#)]
40. Lingfeng, W.; Ying, Q. Near-Infrared Quinoline-Fluoroborodipyrrole Dye: Synthesis and Lysosomal Fluorescence Imaging. *Chin. J. Org. Chem.* **2020**, *40*, 1246–1250.
41. Más-Montoya, M.; Usea, L.; Espinosa Ferao, A.; Montenegro, M.F.; Ramírez de Arellano, C.; Tárraga, A.; Rodríguez-López, J.N.; Curiel, D. Single Heteroatom Fine-Tuning of the Emissive Properties in Organoboron Complexes with 7-(Azaheteroaryl) indole Systems. *J. Org. Chem.* **2016**, *81*, 3296–3302. [[CrossRef](#)]
42. Neese, F. The ORCA program system. *Wiley Interdiscip. Rev. Comput. Mol. Sci.* **2012**, *2*, 73–78. [[CrossRef](#)]
43. van Mullekom, H.A.M.; Vekemans, J.A.J.M.; Meijer, E.W. Band-Gap Engineering of Donor–Acceptor-Substituted π -Conjugated Polymers. *Chem. Eur. J.* **1998**, *4*, 1235–1243. [[CrossRef](#)]
44. Tram, K.; Yan, H.; Jenkins, H.A.; Vassiliev, S.; Bruce, D. The synthesis and crystal structure of unsubstituted 4, 4-difluoro-4-bora-3a, 4a-diaza-s-indacene (BODIPY). *Dyes Pigments* **2009**, *82*, 392–395. [[CrossRef](#)]

-
45. Magde, D.; Wong, R.; Seybold, P.G. Fluorescence Quantum Yields and Their Relation to Lifetimes of Rhodamine 6G and Fluorescein in Nine Solvents: Improved Absolute Standards for Quantum Yields. *Photochem. Photobiol.* **2002**, *75*, 327–334. [[CrossRef](#)]
 46. Goze, C.; Ulrich, G.; Mallon, L.J.; Allen, B.D.; Harriman, A.; Ziesel, R. Synthesis and photophysical properties of borondipyrromethene dyes bearing aryl substituents at the boron center. *J. Am. Chem. Soc.* **2006**, *128*, 10231–10239. [[CrossRef](#)] [[PubMed](#)]